Ferroelectrics as smart mechanical materials

Kumara Cordero-Edwards[1]*, Neus Domingo[1], Amir Abdollahi[2], Jordi Sort[3,4], Gustau Catalan[1, 4]*

[1] Institut Català de Nanociencia i Nanotecnologia (ICN2), CSIC and The Barcelona Institute of Science and Technology (BIST), Campus UAB, Bellaterra, Barcelona 08193, Spain

[2] Laboratori de Càlcul Numèric (LaCàN), Universitat Politècnica de Catalunya (UPC), Campus Nord UPC-C2, E-08034 Barcelona, Spain

[3] Departament de Física, Universitat Autònoma de Barcelona (UAB), Edifici Cc, E-0819 Bellaterra, Spain

[4]Institució Catalana de Recerca i Estudis Avançats (ICREA), Pg. Lluís Companys 23, E-08010 Barcelona, Spain

* Corresponding author:

Email: kumara.cordero@icn2.cat Tel: + 34 93 737 3619

Email: gustau.catalan@icn2.cat Tel: + 34 93 737 3618

Abstract

The mechanical response of homogeneous materials does not change when they are turned upside down, even for piezoelectrics and ferroelectrics. This paradigm can change, however, in the presence of flexoelectricity. Under inhomogeneous deformations, the mechanical response of a ferroelectric depends on its polarity and is therefore switchable. Using nanoindentation, we show that there is a difference in the mechanical response between the two polarities of a uniaxial ferroelectric crystal, that it can be used to quantify its flexoelectricity, and that it enable a fully mechanical reading of the polar orientation of a ferroelectric.

The mechanical responses of homogeneous materials (stiffness, hardness, toughness and so on) are insensitive to space inversion, because all the magnitudes involved (stress, strain, elastic constants) are described by even parity tensors. This mathematical argument is even valid for cristallographically asymmetric materials such as ferroelectrics and piezoelectrics, and physically, this means that the mechanical response of a ferroelectric material should not depend on whether its polar axis is pointing up or down.

However, symmetry restrictions change when deformations are inhomogeneous [1-4]. For example, flexoelectricity (coupling between polarization and strain gradient) allows switching ferroelectric polarization by mechanical means, something that would be otherwise symmetry-forbidden if the strain was homogeneous [5-7]. Flexoelectricity also affects the mechanical response [8-11], and, importantly, the incorporation of strain *gradients* (a third-rank tensor) breaks spatial inversion symmetry, so it allows asymmetric mechanical responses.

Physically, an asymmetric mechanical response could be rationalized by considering the energy cost of deforming a piezoelectric material that generates a polarization $\boldsymbol{P}$ in response to the deformation. This energy cost has two contributions: an elastic one, associated with the deformation itself (Hooke's law), and an electrostatic one, associated with the deformation-induced polarization. The electrostatic energy is $\frac{1}{2}\chi^{-1}P^2$, where χ is the dielectric susceptibility. Because the polarization is squared, the electrostatic energy is insensitive to its sign, and hence turning a piezoelectric crystal upside-down will not make it any softer.

However, when the deformation is inhomogeneous, there are two sources of polarization: the strain itself, via piezoelectricity, and the strain gradient, via flexoelectricity. In a ferroelectric, which is a switchable piezoelectric, these two can be parallel or antiparallel depending on the ferroelectric polarity. Thus, the same inhomogeneous deformation will generate an enhanced polarization when piezoelectricity and flexoelectricity are parallel ($\boldsymbol{P} = \boldsymbol{P}_{piezo} + \boldsymbol{P}_{flexo}$) and a

reduced polarization if they are antiparallel ($\boldsymbol{P} = -\boldsymbol{P}_{piezo} + \boldsymbol{P}_{flexo}$). The depolarization energy still depends on the square of the total polarization ($\boldsymbol{P}^2$), but the *magnitude* of $\boldsymbol{P}$ now depends on the sign of $\boldsymbol{P}_{\text{piezo}}$, so the cost of deformation can in principle become sensitive to polarity.

It is the purpose of this paper to demonstrate that the mechanical response of a ferroelectric is indeed switchable. We show that mechanical asymmetry not only affects toughness, as theoretically predicted [11], but also all other mechanical properties, both plastic and elastic. This discovery, in turn, enables the use of purely mechanical means to quantify flexoelectricity, or to determine the sign of a ferroelectric domain (or, eventually, a ferroelectric memory bit) by just poking it. Both of these concepts are demonstrated here.

We first investigate the mechanical response of ferroelectrics using nanoindentation, which generates flexoelectricity around a sharp indenter tip, as shown in Figure 1(a). The samples studied are single crystals of Lithium Niobate ($LiNbO_3$). We have chosen this material because its ferroelectric phase transition is non-ferroelastic, meaning that only 180° domain switching is possible; this feature prevents any stress-induced ferroelastic reorientation of the polarization [12], thus simplifying the analysis. It is also well-known that, depending on Li^+ concentration, $LiNbO_3$ can be stoichiometric or congruent. The latter has defect dipoles that can introduce an extrinsic asymmetry [13]. Here we have studied samples of both types: stoichiometric and congruent. The stoichiometric sample was single-domain (SLN), so space inversion was achieved by just splitting the crystal in two and turning one half upside-down. The congruent sample was periodically poled (PPLN), so both polarities were accessible on the same side. The results between the SLN and the PPLN crystal were found to be mutually consistent, indicating that sample stoichiometry or switching method do not affect the outcome.

Indentations were first performed in the monodomain crystal, z-cut (i.e., with polarization perpendicular to the surface) and split with one half placed with polarization pointing up and the other pointing down. Both sides were equally polished to mirror-like appearance. In order to get

statistically meaningful results, we performed and analyzed 50 indentations for each mechanical load (25 for each polarity) and measured applying 4 different maximum loads, i.e., a total of 200 indentations. Another set of 100 indentations (50 for each polarity) at a single load were performed on the PPLN. Further details of the nanoindentation measurements are provided in the Methods section, and the full dataset of raw results is provided in the Supporting Online Material.

Figure 1(b) is a schematic of the load-displacement (*F*-*h*) curve for a Berkovich indenter. During the loading process, the material undergoes both elastic and plastic deformation. The total energy related to this process is $U_T = \int_0^{h_{max}} F\,dh$, where h_{max} is the maximum depth reached during loading and *F* is the force applied by the indenter. The elastic deformation is recovered upon unloading; therefore, the elastic energy can be measured as $U_e = \int_{h_f}^{h_{max}} F\,dh$, where h_f is the final indentation depth after complete unloading. Subtracting the total and elastic energies results in the plastic energy $U_p = U_T - U_e$, see the inset in Fig. 1(b).

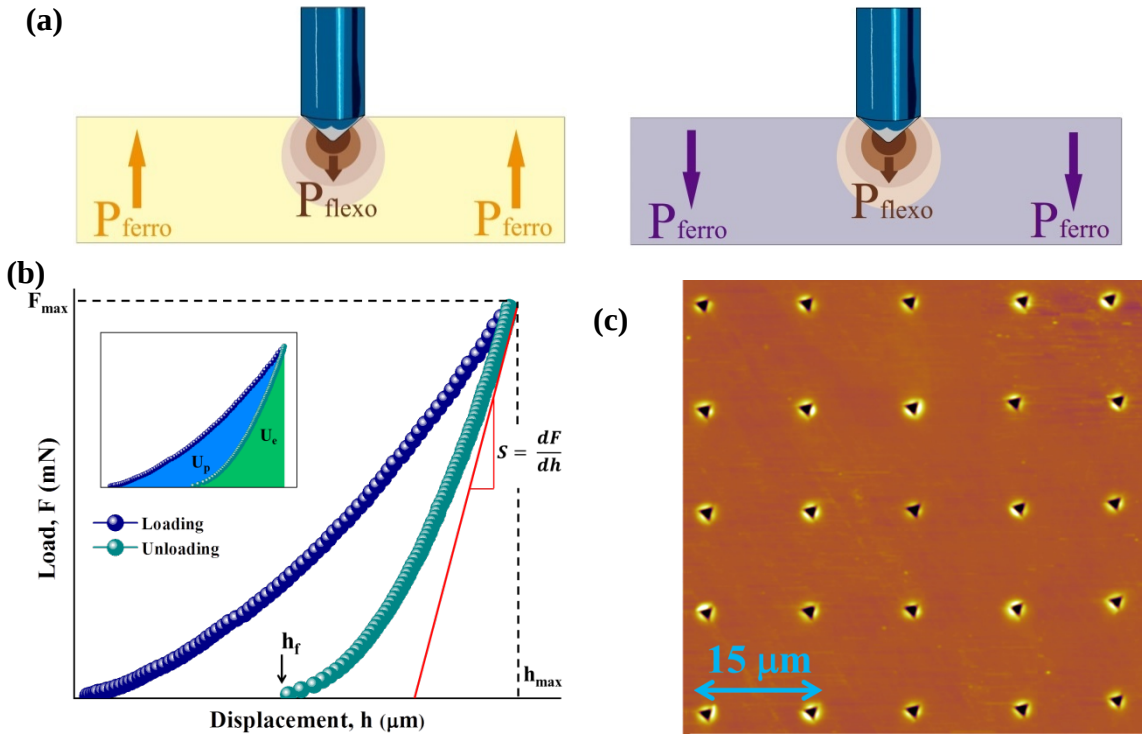

(d)

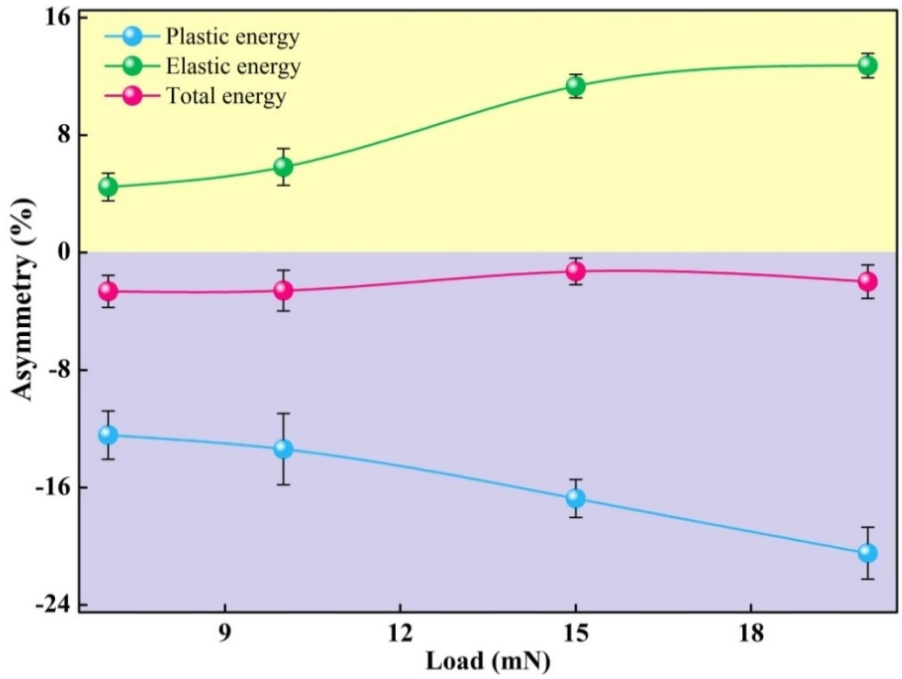

Figure 1: (a) Schematic of the strain gradient field and the associated polarizations (arrows) induced by the indenter tip on a uniaxial ferroelectric with polarization pointing up (left), and polarization pointing down (right). (b) Schematic of the loading and unloading force-displacement curve performed by the nanoindenter, from which the energies (inset), and mechanical parameters are obtained. (c) AFM topography image of the surface of an SLN crystal after performing 25 nanoindentations with the same indentation force. (d) Asymmetry behavior of energies as a function of the applied load in SLN single crystals, showing that both plastic and elastic mechanical responses are asymmetric.

We define asymmetry as $\%Asym \equiv 100\frac{\Delta M}{\langle \acute{M} \rangle}$, where ΔM is the difference between the mechanical indentation energies of the up-polarized and down-polarized states, while $\langle \acute{M} \rangle$ is the mean value. Positive (negative) asymmetry indicates a larger value for the upward (downward) polarization. Figure 1(d) shows the asymmetry of the elastic, plastic, and total indentation energies as a function of applied load. The total energy (elastic + plastic) is symmetric, reflecting that the mechanical energy provided by the indenter is independent of sample polarity, as it should. By contrast, an asymmetric behavior is observed for the plastic energy and thus also by the plasticity index (Figure 1S), which is the dimensionless parameter indicating the ratio of plastic energy to total energy, U_p / U_t. Since fracture toughness is

proportional to the plasticity index [14,15], crack propagation can be sensitive to the sign of polarization [10,11]. Importantly, however, the elastic energy is also asymmetric, and this has profound implications.

The asymmetry of the elastic energy (figure 1(d)) implies that not only plastic but also elastic responses must also be polarity-dependent. Using the Oliver-Pharr method [16,17], we have quantified one plastic and one elastic response: (a) hardness, as a measure of resistance to plastic deformation, and (b) contact stiffness, as a measure of the elastic response of the material. Both are found to depend on polarity (see Figure 1S).

Having demonstrated that flexoelectricity induces mechanical asymmetry, we can now use this asymmetry to quantify the flexoelectric coefficient of ferroelectrics. We do this for two reasons (i) to validate quantitatively that the origin of the asymmetry is indeed the flexoelectric effect and (ii) to demonstrate that flexocoupling coefficients can be measured by mechanical means. In piezoelectrics, finding a new and reliable way to measure flexoelectricity is important because the conventional methods (electromechanical instead of mechanical) yield unrealistically high results [3] due to piezoelectric contributions [18, 19]. We have derived a simplified analytical expression (see Supporting Online Material) relating the flexocoupling coefficient to the difference in free energy (ΔG) between the up and down polarized states:

$$f = \frac{1}{6}\frac{\acute{E}\,\Delta G}{P_0 F} \quad , \qquad (1)$$

where P_0 is the ferroelectric spontaneous polarization (0.8 C/m^2 for $LiNbO_3$ [13]), F is the maximum indentation load and $\acute{E}$ is the average of the elastic modulus measured for the up- and down-polarized states. Experimentally, the energy difference ΔG can be obtained by subtracting the measured elastic energy (area under the unloading curve in Figure 1(b)) of the

upward and downward polar states, i.e. $\Delta G \begin{matrix} -¿ \\ +¿ -U_e^{¿} \\ ¿U_e^{¿} \end{matrix}$. Using the values obtained experimentally and equation (1) the resulting flexocoupling coefficient *f* of SLN is 53.9V, and for PPLN is 39.8V.

The obtained flexocoupling coefficients are still somewhat larger than might be expected from application of the Kogan-Tagantsev criterion, whereby *f* is of the order of <10V [1-3], but the order-of-magnitude agreement is nevertheless remarkable considering the simplifications made in order to obtain a usable analytical expression (see Supporting Online Material). The accuracy also represents an enormous improvement compared to beam-bending experiments, which for ferroelectrics always yield flexocoupling coefficients that are many orders of magnitude too large [3].

Another notable consequence of these results is that they allow determining the polarity of a ferroelectric just by indenting its surface. This is illustrated by contact stiffness measurements performed on PPLN (Figure 3), which show that downward polarized material is stiffer while the upward-oriented one is more flexible.

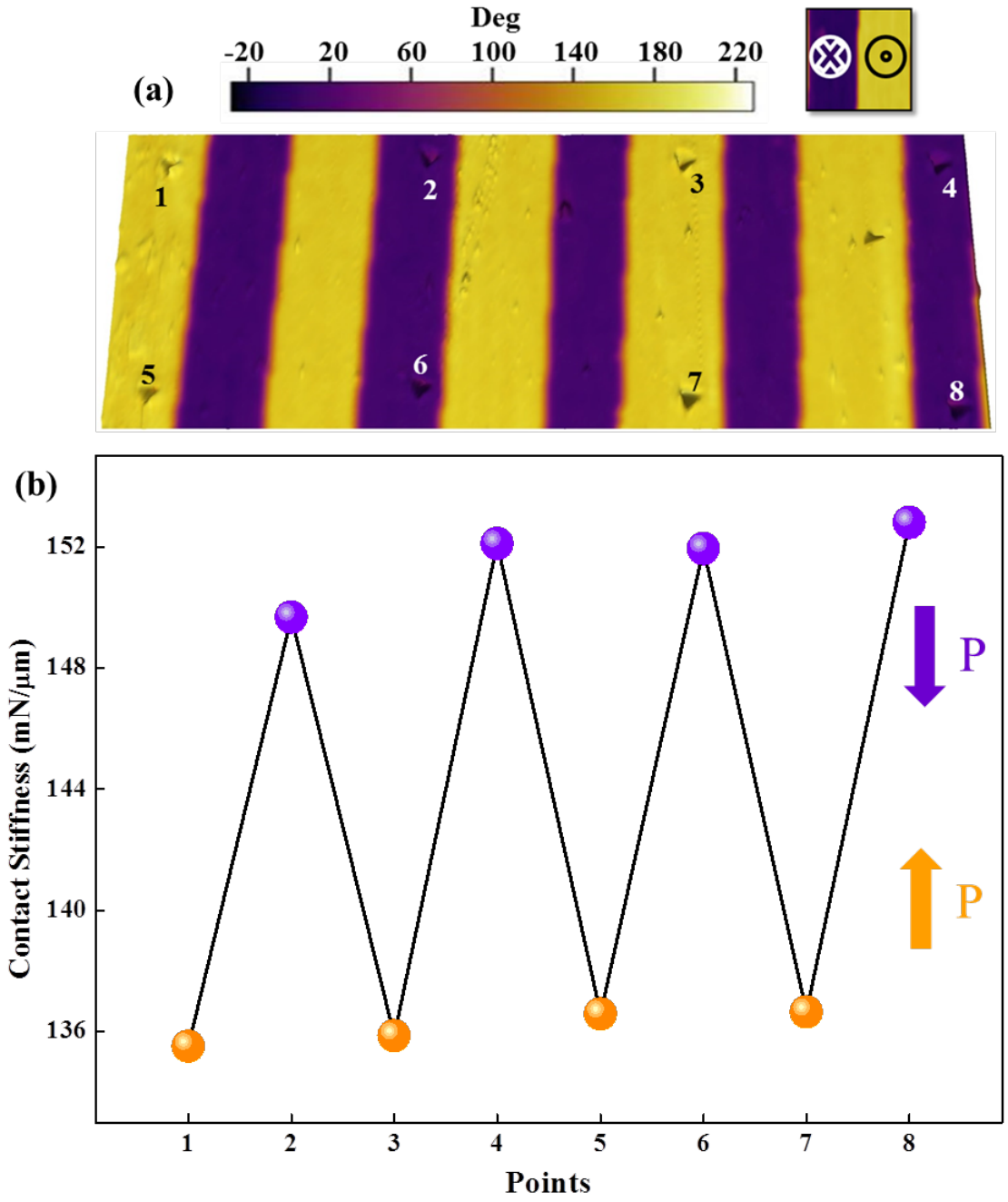

Figure 2: a) 3D plot of topography with superimposed PFM phase image of a few indents performed in PPLN at 7 mN. Yellow means that the polarization is pointing up, whereas purple means that it is pointing down. b) Contact Stiffness measured as a function of the number of indent in (a), showing that the relative stiffness is a direct indicator of a polar state, and therefore it is possible to "read" the polarization of a ferroelectric from its mechanical response.

Nanoindentation is, by definition, a destructive method, but stiffness is an elastic property, so it is not necessary to punch holes in order to read polarity. To prove this point, we use Contact

Resonance Atomic Force Microscopy (CR-AFM) [20] (see Methods): with this technique, we deliver a small oscillatory force with the cantilever of an AFM in order to “tickle” the surface of the ferroelectric, and we monitor the contact resonance frequency of the cantilever coupled to the ferroelectric: the stiffer domains should have higher resonance frequency and the softer domains lower frequency. This technique has been used in the past to evidence contrast between domains of different ferroelastic orientation [21-22], but it was thought to be moot with respect to polar sign due to the arguments stated at the beginning of this article. Our results, however, show that there is in fact a difference in contact resonance frequency, with the down-polarized domains being stiffer than the upward ones, in agreement with the nanoindentation results (Figure 4).

In summary, we have demonstrated that all the mechanical responses of a ferroelectric (both plastic and elastic) to inhomogeneous deformation are asymmetric, and that this asymmetry can be used both to quantify the flexoelectric coefficient itself and to determine the polar sign of a ferroelectric domain. In other words, flexoelectricity makes it possible to read a ferroelectric memory by pure mechanical means. Nowadays ferroelectrics are already considered as smart multifunctional materials on account their switchable polarization and electromechanical response. Our results show that they can also be considered as mechanically smart materials.

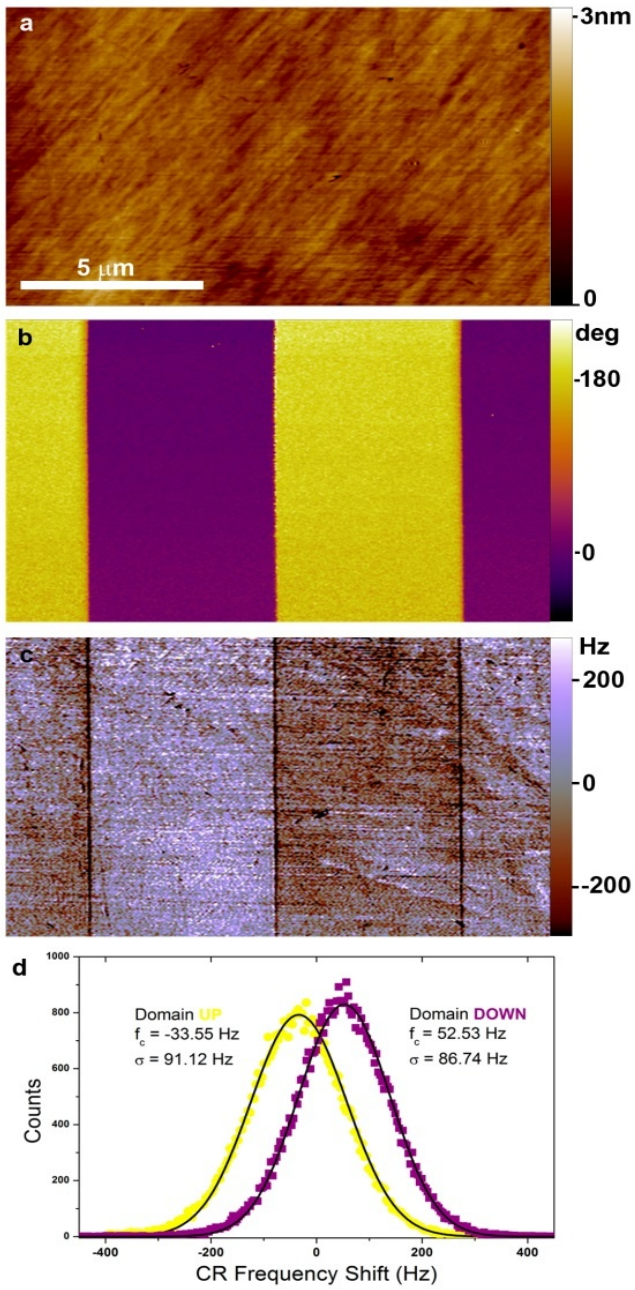

Figure 3: **a**. Topography and **b.** Phase PFM image showing the polarization of the domains in a periodically pooled $LiNbO_3$ sample (PPLN), with Ph_{PFM} = 0º for domains pointing down and Ph_{PFM} = 180º for domains pointing up. **c.** Contact resonance frequency mapping of the PPLN surface, the contact resonance frequency is shifted towards higher frequencies for down-polarized domains, meaning they are stiffer, and to lower frequencies for the up-polarized domains, meaning they are softer. **d.** Histogram of the CR-AFM image shown in **c**: the yellow dots correspond to the frequency shift counts in the areas associated to domains pointing up and purple squares to domains pointing down. Black lines are the corresponding Gaussian fittings, with parameters shown in the inset. The total CR frequency contrast among different polarized domains is of about $\Delta f \sim 86$ Hz, using a cantilever of k ~48 N/m.

Methods

Sample preparation and characterization. Depending on the growth process, single crystals can be *stoichiometric*, with a ratio of 1: 1: 3 for Li^{+}: Nb^{+5}: O^{-2}, or (the most common) *congruent* which exhibit Li^{+} deficiency. Such lithium vacancies can result in defect dipoles that may be either parallel or antiparallel to the ferroelectric polarization, thus introducing an additional and extrinsic source of asymmetry [13] that can complicate the analysis of the results. To guarantee that any evidence of asymmetry originates from flexoelectricity, we use Stoichiometric Lithium Niobate (SLN) single crystals, purchased from MTI Corporation. These are single-domain, so the SLN z-cut single crystal was cut in two equal pieces and we turned one upside-down in order to study two areas with opposite polarization. Both crystals were chemical cleaned. They were sonicated for 15 min in acetone, isopropanol and MilliQ water sequentially. Finally, both were glued in a metallic disc with silver paste, one with the polarization pointing upward and the other downward. We also studied a periodically-poled lithium niobate (PPLN) crystal provided by Asylum Research, Santa Barbara, CA., and chemically cleaned like the SLN. These crystals were congruent; there are no commercially available stoichiometric crystals of PPLN. The polarization of the samples was checked by Piezoresponse Force Microscopy (PFM) using an MFP-3D AFM from Asylum Research, Santa Barbara, CA.

Nanoindentation. Experiments were carried out in the load-control mode, using a UMIS instrument from Fischer-Cripps Laboratories equipped with a Berkovich pyramidal-shaped diamond tip. The thermal drift was always kept below ± 0.05 nms^{-1}. Four different loads (7 mN, 10 mN, 15 mN and 20 mN) were applied. To ensure statistical robustness and accuracy of the results a total of 50 indents per load (25 in each polar state, see Figure 1c)) were performed in the SLN single crystal, and a total of 100 indents per load in the PPLN single crystal. Indents were spaced 15 μm apart (see Figure 1c)), ensuring a sufficient independence of the indents in all cases.

PFM images on PPLN. To correlate the direction of the polarization with each indentation, PFM experiments were carried out, using an MFP-3D AFM, and OMCL – AC240TM – R3 cantilevers, with a k ~ 2 N/m. PFM was mainly operated in DART mode to benefit from resonance signal enhancement; in PFM, an electrical *ac* signal is applied to the tip used as top electrode that excites the sample and mechanical response due to inverse piezoelectric effect is monitored.

CR-AFM images on PPLN. Experiments were carried out using an MFP-3D AFM, in a controlled ambient with N_2. In CR-AFM a mechanical *ac* excitation signal is applied to the cantilever in contact with the surface, and the resonance frequency is monitored, in this case also operating in DART mode. The mechanical resonance of the cantilever in contact with the surface strongly depends on the coupling with the mechanical properties of the surface. Nanosensors NCL Pt coated tips, with k ~ 48 N/m were used. The contact force between the cantilever and the sample was about 25 μN.

Acknowledgements

K. C-E and G.C. acknowledges ERC Starting Grant 308023. Financial support has been obtained under projects from the Spanish Ministerio de Economía y Competitividad (MINECO) under projects FIS2013-48668-C2-1-P and FIS2015-73932-JIN, and the MAT2014-57960-C3-1-R cofinanced by the 'Fondo Europeo de Desarrollo Regional' (FEDER). ICN2 acknowledges support from the Severo Ochoa Program (MINECO, Grant SEV-2013-0295). This work has also been partially funded by 2014-SGR-1015 and 2014-SGR-1216 projects from the Generalitat de Catalunya.

References

1. S. Kogan, *Sov. Phys. Solid State* **1964**, 5, 2069-2079.
2. A. K. Tagantsev. *Phys. Rev. B* **1986,** 34, 5883.
3. P. Zubko, G. Catalán, A.K. Tagantsev. *Annu. Rev. Mater. Res.* **2013**, 43: 387 – 421.
4. R. S. Lakes, R.L. Benedict. *Int. J. Engng Sci.* **1982,** 29, 1161.
5. H. Lu, C. –W. Bark, D. Esque de los Ojos, J. Alcalá, C. B. Eom, G. Catalán, A. Gruverman. *Science* **2012,** 336, 59.
6. Y. Cao, J. Shen, C. A. Randall, L. Q. Chen. *Appl. Phys. Lett.* **2014,** 104, 182905.
7. J. Ocenásek, H. Lu, C. W. Bark, C. B Eom, J. Alcalá, G. Catalan, A. Gruverman. *Phys. Rev B.* **2015**, 92, 035417.
8. M. Gharbi, Z.H. Sun, P. Sharma, K. White. *Appl. Phys. Lett.* **2009,** 95, 142901.
9. C.R. Robinson, K.W. White, P. Sharma. *Appl. Phys. Lett* **2012,** 101, 122901.
10. H. Zhou, Y. Pei, F. Li, H. Luo, D. Fang. *Appl. Phys. Lett* **2014,** 104, 061904.
11. A. Abdollahi, C. Peco, D. Millán, M. Arroyo, G. Catalán, I. Arias. *Phys. Rev B* **2015,** 92, 094101.
12. M.J. Reece, F. Guiu. *Philosophical Magazine A* **2002,** 82, 1: 29-38.
13. S. Kim, V. Gopalan, K. Kitamura, Y. Furukawa. Y. *J. Appl. Phys* **2001,** 90, 2949.
14. G.M. Pharr. *Mater. Sci. Eng. A* **1998,** 253, 151-159.
15. Y. –T- Cheng, C. –M. Cheng. *Appl. Phys. Lett.* **1998,** 73, 614 – 616.
16. W.C. Oliver, G.M. Pharr. *J. Mater. Res.* **1992,** 7, 1564 – 1583.
17. Fisher – Cripps, A.C. Nanoindentation. **2002,** 3rd *Ed. Springer – Verlag*, New York.
18. J. Narvaez, S. Saremi, J. Hong, M. Stengel, G. Catalan. *Phys. Rev. Lett.* **2015,** 115, 037601.
19. A. Biancoli, C.M. Fancher, J.L. Jones, D. Damjanovic, D. *Nat. Mat.* **2015,** 14, 224–229 .
20. U. Rabe, S. Amelio, E. Kester, V. Scherer, S. Hirsekorn, W. Arnold, *Ultrasonics* **2000,** 38, 430-437.
21. U. Rabe, M. Kopycinska, S. Hirsekorn, J. Muñoz-Saldaña, G.A. Schneider, W. Arnold, *J. Phys. D: Appl. Phys.* **2002,** 35, 2621–2635.
22. X. L. Zhou, F.X. Li, H.R Zeng, H. R. *J. Appl. Phys.* **2013,** 113, 187214.